

**Response to PAC Questions on
P906
Proposal for
Drell-Yan Measurements
of Nucleon and Nuclear Structure with the
FNAL Main Injector.**

June 10, 1999

L. D. Isenhower, M. E. Sadler, R. S. Towell
Abilene Christian University, Abilene, TX 79699

D. De Schepper, D. F. Geesaman (Spokesman), B. A. Mueller,
T. G. O'Neill, D. H. Potterveld
Argonne National Laboratory, Argonne IL 60439

C. N. Brown
Fermi National Accelerator Laboratory, Batavia, IL 60510

G. T. Garvey, M. J. Leitch, P. L. McGaughey, J.-C. Peng, P. E. Reimer
Los Alamos National Laboratory, Los Alamos, NM 87545

R. Gilman, C. Glashauser, X. Jiang, R. Ransome, S. Strauch
Rutgers University, Rutgers, NJ 08544

C. A. Gagliardi, R. E. Tribble, M. A. Vasiliev
Texas A & M University, College Station, TX 77843-3366

D. D. Koetke
Valparaiso University, Valparaiso, IN 46383

1 Introduction

At the May 14, 1999 meeting of the FNAL Physics Advisory Committee, we proposed measurements of proton-induced Drell-Yan production on targets of hydrogen, deuterium and heavier nuclear targets at the Main Injector. These measurements will provide precise new information on the ratio of \bar{d}/\bar{u} and $\bar{d} - \bar{u}$ in the proton over the x range of 0.2-0.45, new insight into the non-perturbative origin of the parton distributions and new information on the nuclear dependence of the \bar{u} distributions.

The PAC presented the collaboration with three questions for the June meeting.

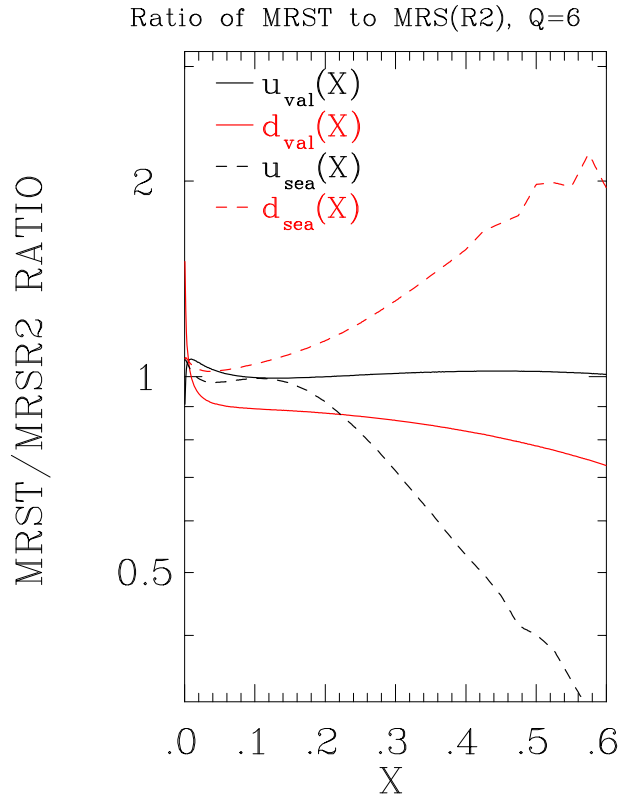
- Did you perform a Monte Carlo simulation of your background trigger rate? Please show in detail all the information that you have been able to collect on this issue.
- Please specify the impact of your proposed measurements on the proton structure functions as a whole, and in particular in the large- x range which is of primary interest for predicting hard processes at current and future high-energy colliders.
- How well would your results compare with competing measurements?

We will first consider the physics questions of the impact of the measurements and possible competing measurements and conclude with the more lengthy discussion of the trigger simulation.

2 Physics impact of the measurements

As we have shown in the PAC presentation, the E866 Deuterium/Hydrogen Drell-Yan results have already had a significant impact on modern parton distribution function (PDF) fits. Figure 1 illustrates the changes between the 1997 vintages of MRS [1] and CTEQ [2] and the 1999 vintages [3, 4]. Figure 2 illustrates the absolute magnitude of each of the MRST light quark distributions. (Note the oscillations in the MRS distributions are a numerical problem with the MRS subroutine. Since this is the standard subroutine from the MRS web site, we have not attempted to change it.) With the inclusion of the E866 data, the individual flavor distributions of the sea have changed by factors of 2 at x of 0.3. The PDF fitters have simply parameterized our data with a convenient algebraic form with little theoretical motivation. The error bars of our E866 determination of \bar{d}/\bar{u} (Figure 3) still allow up to 50% variation at $x = 0.3$ as compared with the few percent errors up to x of 0.4 of the present proposal.

The PDF fits obtain sensitivity to the sea distributions at high x from the CCFR neutrino measurements on iron [5], the E605 Drell-Yan measurements on Cu [6], the E772 Drell-Yan measurements on deuterium [7] and the NA51 [9] and E866 [10, 11] Drell-Yan ratio measurements on deuterium and hydrogen. The E605 and E772 measurements will soon be superseded by E866 absolute Drell-Yan cross section results. The magnitude of $(\bar{d} + \bar{u})$ depends on differences between neutrino, antineutrino and electron/muon deep inelastic scattering results. The nuclear corrections, which can be different for valence and sea quarks, are a significant uncertainty in these comparisons. One of the primary advances of P906 will be absolute p-p Drell-Yan cross sections at high x and a precise measurement of the nuclear dependence of the \bar{u} distribution at these x regions.



Ratio of MRST to MRS(R2) parton distributions at Q=6 GeV.

Ratio of CTEQ5 to CTEQ4 parton distributions at Q=6 GeV.

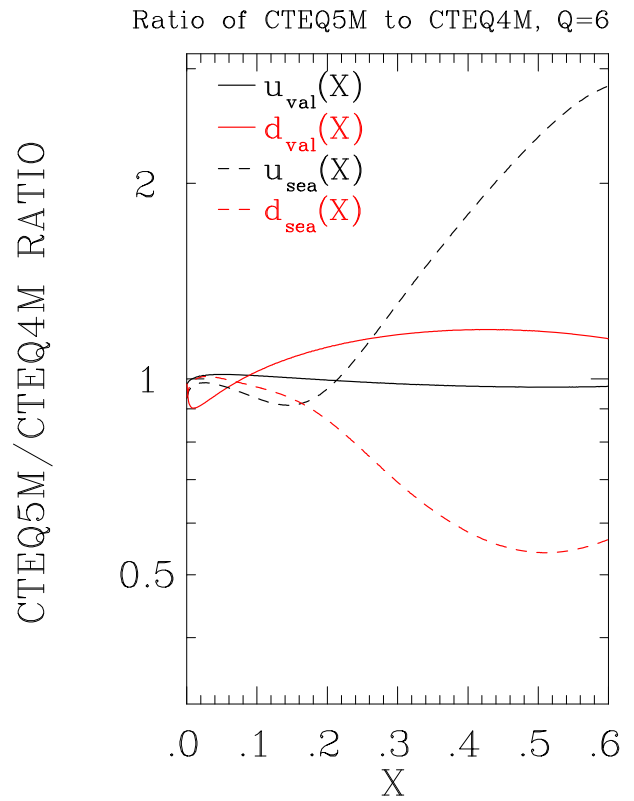


Figure 1: Changes in MRS and CTEQ parton distributions from 1997 to 1999.

The E866 results influenced the fitted valence distributions, primarily the d distribution, through the precise comparison of the Drell-Yan data with the NMC measurements [8] of $F_2^p - F_2^n$. The other new data which have affected the high x valence distributions are the collider W asymmetry data. As is clear from Fig. 2, P906 is sensitive to the region where the antiquarks are numerically small, so we anticipate the P906 measurements will have a relatively small net effect on the valence distributions.

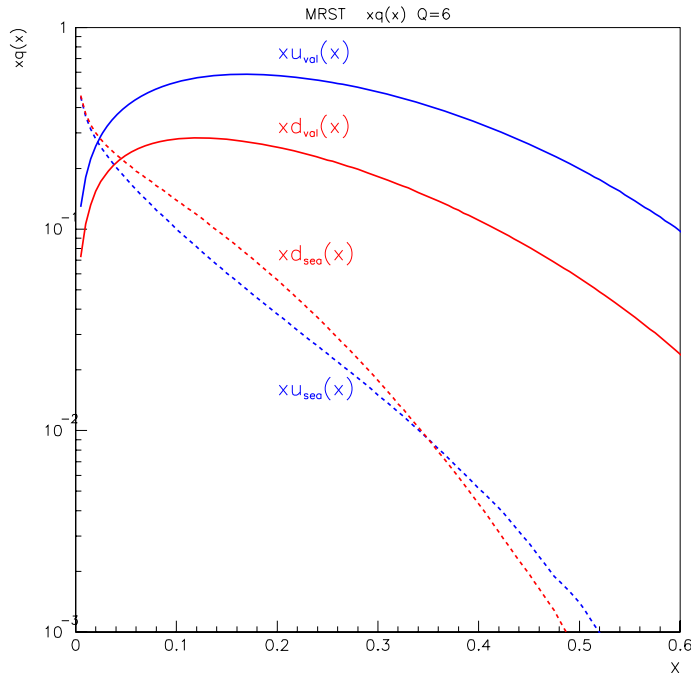


Figure 2: MRST partons distributions at a scale of 6 GeV.

The ultimate impact of the P906 results will be a better handle on the physical mechanism which generates the sea of the proton. Only when we have this fundamental understanding of nucleon structure will we be able to reliably motivate the forms of the parton distributions functions and feel confidence in our ability to extrapolate to unmeasured regions. The large \bar{d}/\bar{u} asymmetry makes it clear that non-perturbative effects dominate the sea distributions at high x . Indeed the collaboration considers this insight into the non-perturbative dynamics a primary motivation of the proposal along with the direct measurement of nucleon structure.

Evolution of the antiquark distributions to high mass scales reveal the differences between the antiquark distribution do not disappear at large scales and the results are sensitive to the assumptions about the x dependence of the antiquark distributions in the unmeasured high x regions. Figure 4 illustrates the ratio of \bar{d}/\bar{u} for MRST (and MRS(R2)) at 6 and 1000 GeV.

For a $\bar{p}p$ collider, the $q\bar{q}$ annihilation diagrams are dominated by the now-well-determined valence distributions at high mass scales. It is unlikely that our proposed measurements will result in significant changes relevant for Tevatron data. For example, W^+ production cross sections change less than 20% when comparing calculations with

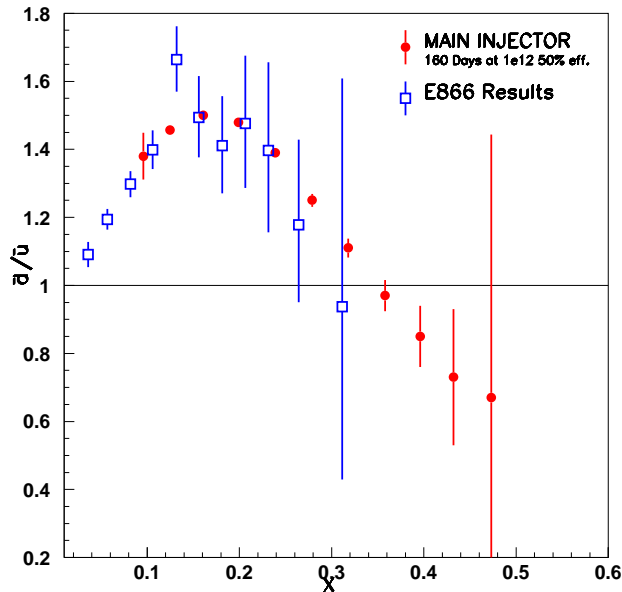


Figure 3: E866 results and projected P906 results for the extraction of \bar{d}/\bar{u} from a 160 day 50% efficiency run with 10^{12} protons per pulse on a 20" long liquid hydrogen and deuterium targets with the P906 apparatus based on the MRST [3] distribution of \bar{d}/\bar{u} .

MRS(R2) and MRST distributions except at the highest rapidities ($y > 2.0$). For a pp collider where boson production cross sections scale like products of distributions such as $u(x_1)\bar{d}(x_2)$ the effect is more dramatic. The yield of high mass events ($M \approx 5$ TeV) at the LHC will vary by factors of two depending on our results. This is within the limits of sensitivity of the LHC for a high mass W' boson with standard coupling and experiments at the design luminosity.

Finally our essentially independent measurements of \bar{d}/\bar{u} from the ratio of yields on deuterium and hydrogen, and $\bar{d} + \bar{u}$ from the absolute cross sections on deuterium provide valuable, albeit indirect, information about the gluon density at high x . Recent work has emphasized the calculational uncertainty in using hadron-induced prompt photon production to determine the gluon distribution due to k_t resummation effects. The $\bar{d} + \bar{u}$ antiquark distribution is intimately linked to the gluon distribution by QCD evolution. One possible explanation of the significant decrease in \bar{d}/\bar{u} for $x > 0.2$ is that the gluon distribution and the symmetric sea is somewhat larger at high x than currently believed. Such an explanation would explain why the deuterium/hydrogen ratio of Υ production cross sections we have measured in E866 is closer to unity than recent PDF (with less high x glue) would predict. A change in the high x gluon distribution would impact, for example, high-transverse-energy jet production at the Tevatron.

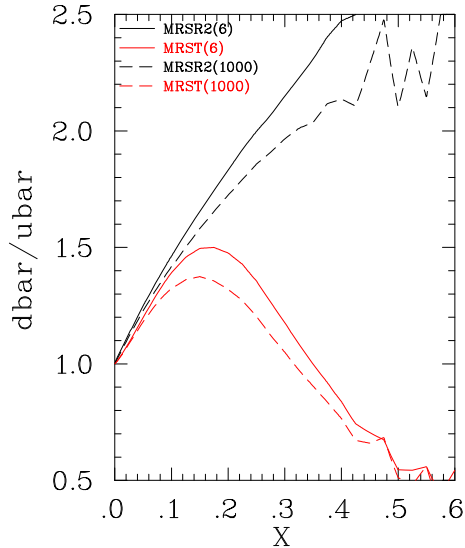


Figure 4: Comparison of MSRT (lower, red) or MRS(R2) (upper, black) parameterizations of \bar{d}/\bar{u} at scales of 6 (solid) and 1000 GeV (dashed).

3 Competing Measurements

We see no significant competition for measurements of the flavor dependence of antiquark distributions in this x range. The classes of experiments with potential sensitivity are neutrino deep inelastic scattering (DIS), semi-inclusive deep inelastic scattering (SIDIS), electroweak boson production at pp colliders and other Drell-Yan measurements. We will briefly consider each of these in turn.

CCFR has accumulated significantly more statistics in neutrino and antineutrino DIS which will allow a more precise determination of $(\bar{d} + \bar{u})$ but the uncertainties of using a heavy target will remain. On an almost isoscalar target, there is little sensitivity to $(\bar{d} - \bar{u})$. SIDIS uses the flavor dependence of the parton fragmentation functions to untangle the contributions of the different parton distributions. The HERMES collaboration at DESY has used SIDIS to study the flavor dependence of the sea [12]. The HERMES results agree well with the E866 results but have factors of 5 larger error bars. SIDIS most directly measures

$$\frac{\bar{d}(x) - \bar{u}(x)}{u(x) - d(x)} = \frac{J(z)[1 - r(x, z)] - [1 + r(x, z)]}{J(z)[1 - r(x, z)] + [1 + r(x, z)]}$$

$$r(x, z) = \frac{N_p^{\pi^-} - N_n^{\pi^-}}{N_p^{\pi^+} - N_n^{\pi^+}}$$

where $J(z)$ depends on the fragmentation functions and z is the fraction of the energy of the virtual photon carried by the hadron. At high x where the difference of antiquark distributions is much smaller than the difference of quark distributions, one must measure differences of several comparable size numbers. Additionally, the systematic uncertainty due to the fragmentation physics is also an issue. The experiments which can improve

these measurements are HERMES and COMPASS, both of which concentrate on polarized structure function measurements. While HERMES will likely increase their data set by another factor of five in dedicated unpolarized running, they will not be able to extend their x range significantly to higher x . The COMPASS experiment at CERN could do similar semi-inclusive SIDIS measurements. To date they have not proposed dedicated unpolarized running with rapid interchange of pure hydrogen and deuterium targets.

W production in p-p collisions does offer sensitivity to the antiquark distributions. At the LHC one only has sensitivity for the x range considered here at the highest rapidities (> 4). However at RHIC higher x values are quite relevant and plans are underway to use the W decay asymmetry in single spin asymmetries to study the antiquark polarization. Since the RHIC detectors have limited kinematic coverage and these events have missing transverse energy, the parton level kinematics of each event are not well determined and one averages over a significant x region. With the antiquark distributions falling rapidly, the lepton asymmetry yields are dominated by lower x values. We have discussed the plans with members of the STAR and PHENIX collaborations at RHIC. They concluded that they will not be sensitive to the antiquark distributions at $x > 0.2$.

In contrast to processes like SIDIS, the Drell-Yan measurement of \bar{d}/\bar{u} has much smaller systematic errors and acceptance corrections. We know of no other planned fixed target Drell-Yan measurements in the near future. In the long term, lower energy, high intensity machines such as the Japanese hadron facility could address this physics. We consider the energy of the main injector to be the optimum combination of reliable interpretation and attainable precision.

Experts like James Sterling [13] have given their strongest support to our proposal as the best way to measure the flavor dependence of the antiquark distributions at high x . Again we see no serious competition for this experiment in the near future.

4 Signal and Background Trigger Rates

As described in the P906 Proposal, the Monte Carlo code that has been used to estimate trigger rates is a modified version of the “Fast Monte Carlo” that was written many years ago to estimate acceptances for the Meson East Spectrometer. For P906, the code has been modified to make the spectrometer configuration more flexible and to include additional muon generators. This Monte Carlo simulates muons from Drell-Yan scattering, resonance production (J/ψ , ψ' , Υ , Υ' , Υ''), and π , K and charmed meson decays. It can track either single muons or pairs through the spectrometer magnets and detector stations. The Fast Monte Carlo simplifies the treatment of the magnetic field, for example treating the proposed 189” long magnet as a sequence of nine separate 21” long uniform field segments. In contrast, it provides full simulation of the energy loss and multiple scattering distributions of the muons as they pass through the beam dump, absorber and detector materials, using the same subroutines that are used in the primary E866 Monte Carlo code. It also simulates the traceback of muons from the detector stations through the magnets and absorber materials to the target so that realistic tracking cuts may be imposed and the ultimate resolutions of the spectrometer can be estimated.

To optimize simulation speed, the philosophy behind the event generators is to throw

events according to kinematic distributions that will enhance the probability that the subsequent muon tracks will pass through the system successfully. The thrown events are then weighted according to the cross section times target thickness for the kinematics as generated, relative to the probability of throwing that kinematics. For example, Drell-Yan events are typically thrown with a uniform distribution in mass (from 3-10 GeV when simulating pair triggers and from 1.15-10 GeV when simulating background single muon tracks originating from Drell-Yan scattering) and with a Gaussian x_F distribution with a mean of 0.2 and a sigma of 0.3, truncated at $x_F = \pm 1$. For each event that passes through the spectrometer successfully, the true $d^2\sigma/dMdx_F$ is calculated using the leading-order Drell-Yan cross section formula and the MRST parton distributions, together with a K factor that has been determined by comparing leading-order and next-to-leading-order Drell-Yan cross section calculations. This true cross section determines the weight for the event. The J/ψ and ψ' calculated cross sections are based on measured production rates at $x_F = 0$ and the x_F dependence predicted by the color evaporation model. The Υ cross sections are only rough approximations, but they are quite adequate since few Υ events are expected over the life of P906. The p_T distributions of thrown Drell-Yan and resonance events are taken from the measured p_T dependence of $\bar{p}p \rightarrow J/\psi X$ at 125 GeV.

The $D\bar{D}$ cross section has been extrapolated from higher energies to 120 GeV. The x_F and p_T distributions of the individual D 's have been estimated from higher-energy measurements, and then artificially stiffened substantially in order to compensate for difficulties in extrapolating the $D\bar{D}$ physics to 120 GeV. The x_F and p_T values are chosen independently for the two D 's, consistent with crude constraints from energy and momentum conservation. The azimuthal directions of the two D 's are assumed to be exactly 180° apart. Therefore, the Monte Carlo estimates for both single muons and muon pairs from charm production are likely to be overestimates of the actual rates that we will encounter during P906.

Large numbers of mesons (π 's, K 's) will be produced by the beam as it travels through the target and as it is attenuated in the dump. Some of the mesons will decay into muons before being absorbed in the dump. The π and K production cross sections were estimated using the parameterization of Anthony Malensek (FN-341 and followup report). Mesons were thrown flat in longitudinal momentum and production ϕ and were thrown with the Malensek distribution for $|P_t|$. In the simulation for target production, the mesons were tracked until a randomly determined position between the production point and the dump, decayed, and then tracked through the rest of the simulation as muons. In the simulation for dump produced mesons, the production point was determined using the solution of the coupled differential equation for proton attenuation and meson production and attenuation. Each muon was tracked through the spectrometer and weighted by the product of the production cross section, decay probability, and branching fraction into muons.

The Monte Carlo code has been verified through a number of tests. It gives a reasonable description of the rates that were observed during E866. For P906, its prediction of the flux of muons with momenta above 3 GeV/ c that should be present at Station 1 is consistent with a full GEANT simulation of the target, beam dump, magnet and absorbers. The simplified muon traceback to the target has been checked by verifying that it reproduces observed resolutions during E866. For example, the predicted and

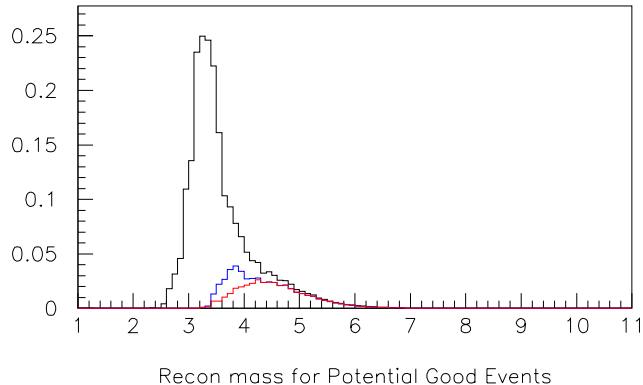


Figure 5: The reconstructed mass spectrum (in GeV/c) of real pairs from the target after tracking cuts have been applied to each muon. The top (black) curve is the expected mass spectrum with the trigger track selection criteria that were used when writing the P906 proposal. The middle (blue) curve is the expected mass spectrum with the new trigger track selection criteria that have been developed since then. The lower (red) curve is the contribution of Drell- Yan pairs to the new expected mass spectrum.

observed J/ψ mass resolutions during the E866 large- x_F nuclear dependence study agree to within 10%.

The Monte Carlo is used to identify those scintillator hodoscope roads through the spectrometer that are associated with the Drell-Yan pairs in which we are interested. The various background processes are then simulated to determine the rates of single muon tracks and real pairs that will pass through the same scintillator hodoscope roads. The random muon pair trigger rates are calculated from the predicted single muon trigger rates. Signal and background event rates are then estimated by requiring the reconstructed tracks to pass typical analysis cuts that we will apply to eliminate, for example, interactions in the beam dump.

The rates quoted in the P906 proposal were based on an early set of scintillator hodoscope roads. Since the proposal was written, we have continued to optimize the track selection criteria of the hardware trigger. The current track selection criteria reduce the background trigger rates substantially, while keeping nearly all of the most interesting Drell-Yan muon pairs. This is illustrated in Figs. 5, 6 and 7. Figures 5 and 6 show the expected reconstructed mass spectra of real pairs from the target that pass all tracking cuts for the previous trigger configuration and the new one. The new configuration reduces the trigger rate due to charmonium resonances by a factor of 15. The trigger rate due to Drell-Yan pairs is reduced by 45%, but most of the pairs that fail the new trigger configuration would not have been useful in any case since they have reconstructed masses below 4.2 GeV and could be confused with muon pairs from ψ' decay. Figure 7 shows the x_2 distributions of the Drell-Yan muon pairs with reconstructed masses between 4.2 and 8.8 GeV that pass all tracking cuts for the previous trigger configuration and the

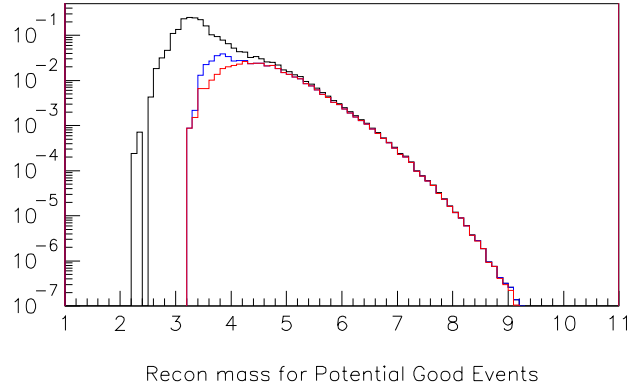


Figure 6: Identical to Fig. 5, but with a logarithmic scale.

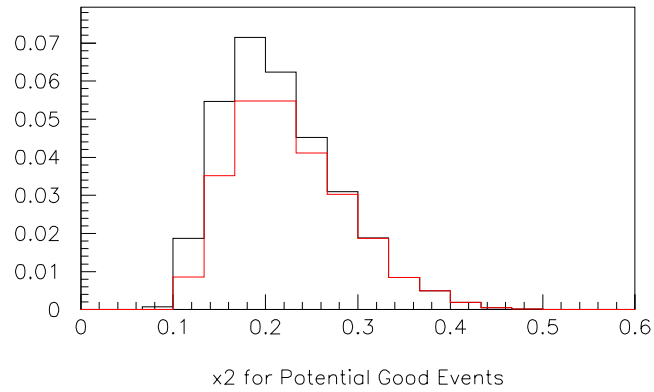


Figure 7: The x_2 spectrum for Drell-Yan pairs that pass all tracking and reconstructed mass cuts. The upper (black) curve is the expected x_2 distribution with the trigger track selection criteria that were used when writing the P906 proposal. The lower (red) curve is the new expected x_2 distribution. The vertical scale is in units of 10^6 counts per x bin.

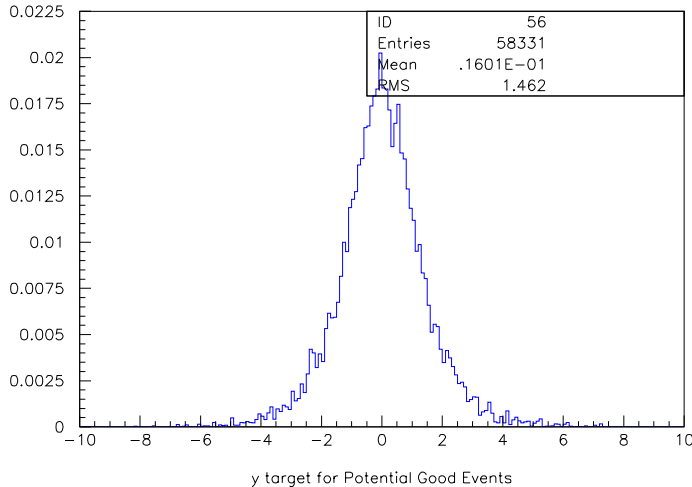


Figure 8: The Y_{target} distribution (in inches) for muons from Drell-Yan pairs when the pair passes the reconstructed mass cut and all tracking cuts, except the cut $|Y_{target}| \leq 3$ for the muon shown.

new one. The new configuration leads to a 30% reduction in the total yield for $x_2 < 0.2$ and a 10% reduction for $0.2 < x_2 < 0.267$. The reduction in the yield for $x_2 > 0.267$ is less than 1.5%.

Given this revised set of trigger hardware track selection criteria, we will undoubtedly choose to run for a short period of time with low beam intensity at a lower main spectrometer magnetic field setting to provide good coverage of the J/ψ and ψ' region, together with the low mass part of the Drell-Yan continuum. This follows the strategy used by E772 and E866 of using different magnet settings to optimize the Drell-Yan acceptance at different masses, then adjusting the beam intensity to optimize the trade-off between statistics, the real:random rate and rate-dependent reconstruction problems.

Figures 8, 9 and 10 show the tracking cuts that have been adopted. Y_{target} and X_{target} are calculated by finding where the reconstructed track crosses the plane at the center of the target. The y resolution is worse than x for two reasons. The vertical angular range of the spectrometer is much larger than the horizontal range, increasing the error due to the assumption that all events originate at the center of the target. Also, tracks on the tail of the absorber energy loss distribution are tracked through the spectrometer with too low a momentum and subsequently deflected too much in the first magnet. Y_{dump} is calculated by finding where the reconstructed track crosses the plane $z = +6''$, the mean interaction point of the beam in the Cu dump. The Y_{dump} cut serves two purposes. Most importantly, when combined with the target cuts, it rejects nearly all tracks that actually originate in the dump, rather than the target. Meanwhile, it also eliminates most muons from the target that pass through a substantial length of the Cu beam dump and therefore have poor resolutions. The expected effective mass and x_2 resolutions for Drell-Yan pairs that pass all cuts are shown in Figs. 11 and 12.

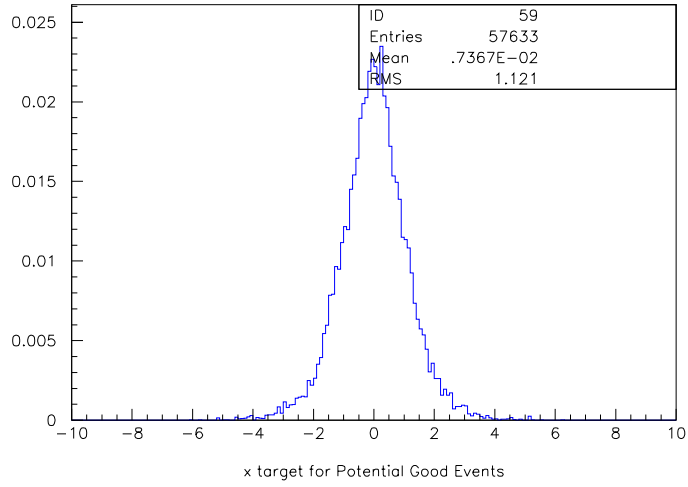


Figure 9: The X_{target} distribution (in inches) for muons from Drell-Yan pairs when the pair passes the reconstructed mass cut and all tracking cuts, except the cut $|X_{target}| \leq 3$ for the muon shown.

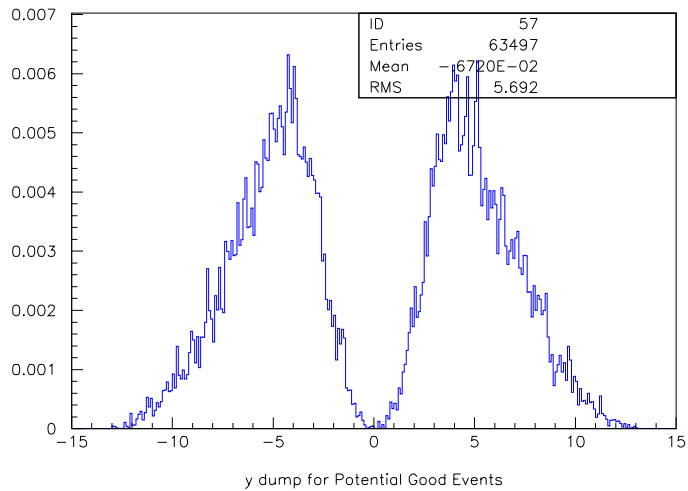


Figure 10: The Y_{dump} distribution (in inches) for muons from Drell-Yan pairs when the pair passes the reconstructed mass cut and all tracking cuts, except the cut $|Y_{dump}| \geq 2.5$ for the muon shown.

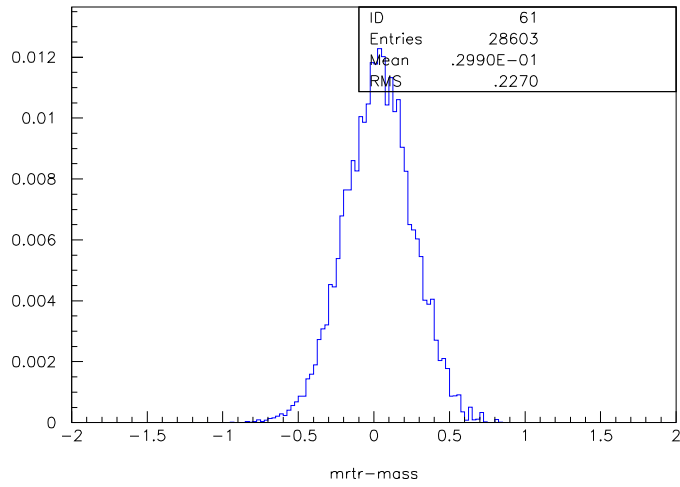


Figure 11: The difference (in GeV) between the reconstructed and true dimuon masses for Drell-Yan pairs that pass the trigger and all cuts.

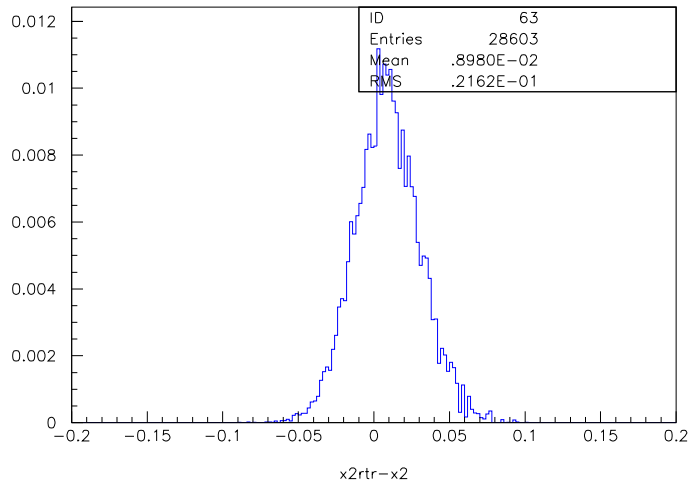


Figure 12: The difference between the reconstructed and true x_2 for Drell-Yan pairs that pass the trigger and all cuts.

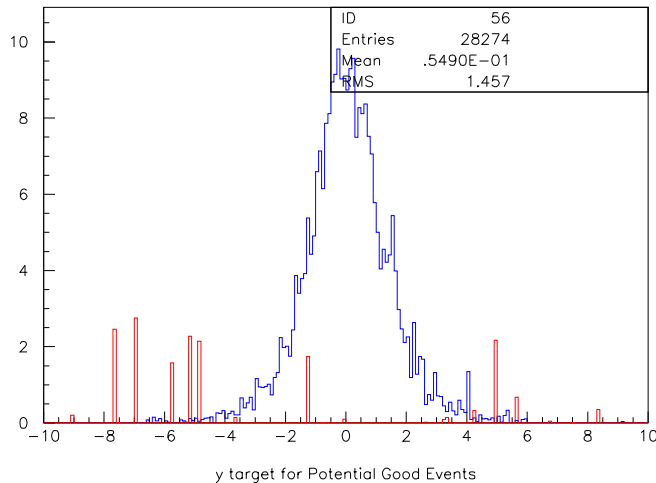


Figure 13: The Y_{target} distribution (in inches) for single muons originating from Drell-Yan, resonance or open charm production in either the target (blue) or dump (red) that pass the trigger and the X_{target} and Y_{dump} cuts.

We have used the Monte Carlo to estimate the trigger rates. The rates of real muon pairs from Drell-Yan and resonance production originating in either the target or the dump have been simulated for the equivalent of 10^3 to 10^5 spills at an assumed intensity of 10^{12} protons per spill. The rate due to Drell-Yan pairs off the LH_2 target is 0.53/spill, with half of these passing the tracking and effective mass cuts. The total rate is expected to be between 8 and 9 events/spill, depending on the target. Approximately 75% of this originates from Drell-Yan pairs produced in the beam dump. The yield of muon pairs from $D\bar{D}$ production is negligible.

The singles muon rates due to all of the above processes have also been estimated. The rate due to Drell-Yan scattering in the target has been simulated for the equivalent of nearly 100 spills, while those due to resonance and open charm production have been simulated for the equivalent of several 10's of spills. Detection of muons produced via Drell-Yan, resonance and open charm production in the beam dump have been simulated for the equivalent of approximately 10 spills. The trade-off between target and dump events has been chosen to provide reasonable statistics in all cases and very good statistics for those events that might reconstruct as target events – since those are the events that will contribute to the random background after analysis cuts have been applied. Figures 13, 14 and 15 show reconstructed track distributions for single muons from Drell-Yan, resonance and open charm production in either the target or the dump. As in Figs 8 to 10, tracks are only included in a spectrum if they pass all the other tracking cuts. Very few dump events appear in Figs. 13 and 14 because most fail the $|Y_{dump}| \geq 2.5''$ cut, as illustrated by Fig. 15.

Given the enormous number of muons from π and K decay, it has been impractical to date to simulate the backgrounds due to those processes for the equivalent of more than a

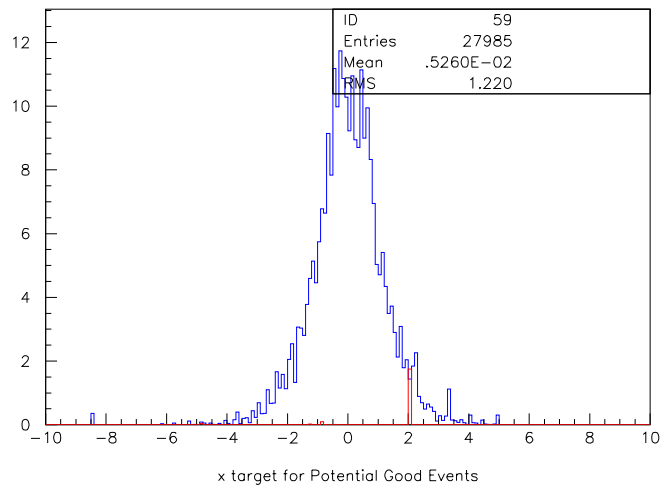


Figure 14: The X_{target} distribution (in inches) for single muons originating from Drell-Yan, resonance or open charm production in either the target (blue) or dump (red) that pass the trigger and the Y_{target} and Y_{dump} cuts.

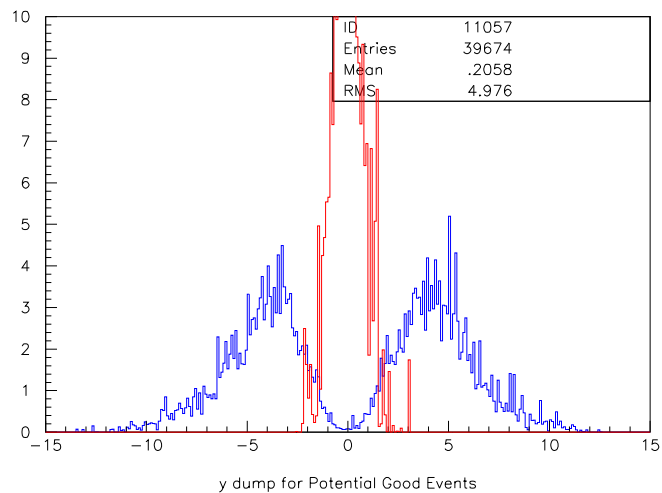


Figure 15: The Y_{dump} distribution (in inches) for single muons originating from Drell-Yan, resonance or open charm production in either the target (blue) or dump (red) that pass the trigger and the Y_{target} and X_{target} cuts.

small fraction of a beam spill, even though the statistics have been increased by a factor of 4 since the proposal was submitted. The estimated rates from π and K decay are due primarily to a very small number of events with very large weights (several hundred) that successfully passed the trigger, and later the tracking cuts as well. These are sufficient to estimate the ultimate yield with a substantial statistical uncertainty, but only provide a very qualitative view of the detailed tracking distributions. The tracking distributions appear similar to those in Figs. 13 to 15, after accounting for the asymmetries that appear for Y_{target} and Y_{dump} due to the prevalence of positive over negative muons from π and K decays. We have now determined the kinematic regions in which muons from π and K decay preferentially pass the hardware trigger, and we are planning to adjust the parameters of the π and K decay generator to throw a considerably higher fraction of the total events in those regions. This will give us much better statistics for the events of interest to us in the near future. In the meantime, the estimates below are based on the statistics obtained to date.

When running with the liquid hydrogen target, the primary source of background single muons will be π and K decay-in-flight in the beam dump. When running with the liquid deuterium target, the π and K decay-in-flight background from the target is predicted to be slightly larger than that from the dump. The total single muon trigger rate is predicted to be ≈ 46 KHz with the LH_2 target and ≈ 62 KHz with the LD_2 target. In each case, the Monte Carlo predicts that we should see approximately 2/3 positive muons and 1/3 negative muons. To obtain a conservative estimate of the trigger rate, we have chosen to double the predicted rates of true single muon triggers in order to account for random contributions to the single muon rate and finite duty-factor of the proton beam when estimating the random pair rates. This leads to estimates of 55 random di-muon triggers per spill for the LH_2 target and 105 random triggers per spill for the LD_2 target, counting all random opposite-sign pairs and the random like-sign pairs that have one muon on each side of the spectrometer.

As noted in the P906 proposal, we also expect to take approximately 80 study triggers per spill – including prescaled single muons to study the random background, triggers to monitor the efficiency of the hodoscopes, and triggers to investigate any rate-dependence that may be present in the data analysis. Thus, we now have a conservative estimate of approximately 200 triggers or less per spill. This will be very straightforward, given that the data acquisition system will be capable of handling well over five times that rate.

We have also estimated the number of single muon tracks per spill that will satisfy the tracking cuts in addition to the trigger. These are the muon tracks that might lead to random coincidences that will pass our analysis cuts. We expect approximately 6500 muons to pass the trigger and tracking cuts for 10^{12} protons incident on the LH_2 target, and twice that for the LD_2 target. The dominant source of muons is decay-in-flight of π 's and K 's produced in the target. Again, the majority of the muons are positive. This leads to a real-to-random ratio of 5 to 1 for the LH_2 target, averaged over all effective masses of the muon pair. The mass spectrum of the random muons is strongly peaked at low effective masses. This is illustrated by a comparison of the Y_{dump} distributions in Figs. 10 and 15. The RMS Y_{dump} values can be seen to be 5.7 for Drell-Yan pair events and 5.0 for the single muon background events from the target that passed all other trigger and tracking cuts. This difference leads to a smaller muon pair opening angle distribution for randoms, which translates directly into a softer mass spectrum. We must cut low mass

pairs during analysis, in any case, due to ψ' contamination of the Drell-Yan continuum. That cut will improve the the real-to-random ratio for the Drell-Yan events of interest, compared to the overall average. Therefore, we anticipate that, after full analysis cuts, the LH_2 target real-to-random ratio for will be better than 6 to 1 at all x_2 values, and much better than that at intermediate and large x_2 . The real-to-random ratio off LD_2 at any given x_2 value will be half of that off LH_2 .

References

- [1] A. D. Martin, R. G. Roberts and W. J. Stirling, Phys. Lett. B **419**, 1280 (1997).
- [2] H. L. Lai *et al.*, Phys. Rev. D **55**, 1280 (1997).
- [3] A. D. Martin, R. G. Roberts, W. J. Sterling and R. S. Thorne, Eur.Phys.J. **C4**, 463 (1998).
- [4] H. L. Lai *et al.*, hep-ph/9903282 (1999).
- [5] W. G. Seligman *et al.* Phys. Rev. Lett. **79**, 1213 (1997).
- [6] G. Moreno *et al.*, Phys. Rev. D **43**, 2815 (1991).
- [7] P. L. McGaughey *et al.* Phys. Rev. D **50**, 2038 (1994).
- [8] P. Amaudruz *et al.*, Phys. Rev. Lett. **66**, 2712 (1991); M. Arneodo *et al.*, Phys. Rev. D **55**, R1 (1994).
- [9] A. Baldit *et al.*, Phys. Lett. B **332**, 244 (1994).
- [10] E866 Collaboration, E. A. Hawker *et al.*, Phys. Rev. Lett, **80** 3715 (1998).
- [11] E866 Collaboration, J.-C. Peng *et al.*, Phys. Rev. D **58**, 092004 (1998).
- [12] K. Akerstaff *et al.*, Phys. Rev. Lett. **81**, 5519, (1998).
- [13] J. Sterling, Letter to John Peoples, May 1998.
- [14] A. D. Martin, W. J. Stirling and R. G. Roberts, Phys. Lett. B **252**, 653 (1990).
- [15] C. A. Gagliardi *et al.*, Nucl. Instrum. Methods A **418**, 322 (1998).